

EXPERIMENTAL AND THEORETICAL STUDIES
OF THE BREADTH AND STRUCTURE
OF THE
COMPTON SHIFTED LINE.

Thesis

by

Jesse W. M. DuMond.

In partial fulfillment of the requirements for
the degree of Doctor of Philosophy.

California Institute of Technology,
Pasadena, California.

1929.

TABLE OF CONTENTS.

Part I - Experimental.

	page
Introduction.	1
Experimental causes of the breadth of the shifted line.	2
The effect of a scattering angle of approximately 180° .	3
The target spectrometer.	6
Details of technique.	7
Exposures.	18
Analysis of films.	19
The experimental curves.	24

Part II - Theoretical.

The relation between Compton line structure and electron velocity distribution.	27
General method of computing and normalizing line structure curves.	32
Line structure curve due to Sommerfeld conduction electrons.	35
Line structure curve due to Maxwell-Boltzmann distribution of conduction electron velocities.	36
Line structure curves for Kepler orbital velocity distribution.	37
Conclusion.	38
Appendix.	43
Summary.	48
References.	49

PART I.

EXPERIMENTAL.

INTRODUCTION.

In October 1922, Arthur Compton discovered that monochromatic X radiation when scattered by elements of low atomic number contains longer wave lengths not originally present before scattering in addition to the initial primary line. This "softening" by scattering had been observed previously by absorption methods in a qualitative way, but Compton's discovery consisted in showing quantitatively the precise nature of this shifted radiation, namely, that it appeared as a rather broad diffuse "line" differing in wave length from the primary line by a wavelength difference of

$$\Delta\lambda = \frac{h}{m c} (1 - \cos \theta) = 24 \cdot 10^{-11} (1 - \cos \theta)$$

Subsequently other investigators, Compton and Woo, Webster, Ross, Becker, Sharp, Allison and Duane, Danvillier and many others obtained both by photographic and ionization chamber methods definite evidence for the existence of the "shifted" line. Almost invariably this shifted line has appeared broader and more diffuse than the unshifted line which almost always accompanies it. The primary line generally used is the $K\alpha$ doublet with a separation between its components of 4 X.U.. The author knows of only one case in which this doublet appears even faintly resolved in the shifted position though it is almost always partially resolved in the unshifted positions. This exceptional case is a photograph taken by Ross of the scattered radiation

from a molybdenum target with aluminum as the scatterer. This photograph remains unexplained today. It has not been reproduced.

EXPERIMENTAL CAUSES OF BREADTH OF THE SHIFTED LINE.

The diffuse nature of the shifted line may either be ascribed wholly to experimental causes or it may be in part at least a natural breadth whose explanation must be sought in the process of scattering itself. Possible experimental causes are,

1. Imperfections in the analyzing crystal.
2. "Cross fire" (especially when combined with imperfections or distortions of the analyzing crystal). By "cross fire" is meant the presence of rays whose reflection angles at any one point on the crystal lie in planes not mutually parallel. When the source of the radiation falling on the analyzing crystal is virtually a point cross fire is unimportant. With an extended source it assumes considerable importance. Consider for example a scattering body the source of scattered radiation sending radiation under the wedge of a Seeman type crystal spectograph with a wedge length somewhat less than the dimensions of the scatterer. Evidently every point on the photographic negative receives radiations from the entire height of the crystal over the full length of the wedge. Those rays reflected under the wedge in a plane normal to the wedge will form a spectral line on the negative in a slightly different position from those reflected in planes oblique to the wedge. With a point

source this effect gives the spectral lines a slight curvature. They are in fact short segments of hyperbolae. With an extended source however the superposition of all such hyperbolic segments from all the points of the source results in a broadened line. Furthermore, if the crystal is imperfect either naturally or due to elastic strains introduced in mounting, a point source will give a slightly crooked line while an extended source will give a broadened line. The result of translating such a crooked line along the general direction of its own length.

3. Inhomogeneity of scattering angle. Since the shift is known to depend on the scattering angle, inhomogeneity of scattering angle will result in inhomogeneity of shift and a consequent broadening of the shifted line.

Of the three causes listed above evidently 1 and 2 affect the unshifted line to the same extent as the shifted line. They are not therefor sufficient to explain the greater breadth of the shifted line. As a matter of fact the writer has succeeded in obtaining unshifted scattered lines as sharp as the primary lines from a point source and the explanation for the diffuse unshifted so frequently observed is to be found under either cause 1 or cause 2. Cause 3, however, must be eliminated before the diffuse character of the shifted line can be established as an intrinsic effect of scattering.

THE EFFECT OF A SCATTERING ANGLE OF APPROXIMATELY 180° .

Since the shift is proportional to $(1 - \cos \theta)$ where θ is the scattering angle the shift is evidently a maximum when $\theta = 180^\circ$.

From a consideration of the accompanying figure (1) it becomes evident that in the vicinity of $\theta = 180^\circ$ the inhomogeneity of shift due to a given inhomogeneity of scattering angle is reduced to a very small minimum. There are thus two reasons why this region is a desirable one for the study of Compton line structure.

On the other hand, the region near 180° is a difficult one to attain. Evidently exactly 180° is unattainable for here either the source of primary radiation interferes with the returning scattered

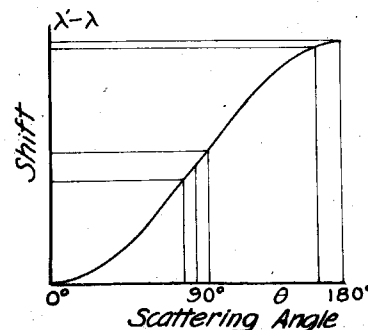


Fig. 1

beam or the spectrometer interferes with the primary beam. The primary radiation is many thousand times more intense than the spectroscopically analysed scattered radiation. Evidently then with large angles of scattering very serious difficulties arise from the necessity of completely screening off this very intense primary radiation which would otherwise completely mask the spectrum to be studied.

Inhomogeneity of scattering angle is unavoidable because the primary radiation incident on the scatterer coming from the source of X rays in order to possess any finite intensity must subtend a finite solid angle at the source.

The great loss of intensity in the scattering process and in the subsequent spectral analysis makes very long exposures necessary even when any intense primary radiation is used. It is therefor desirable to have a maximum primary X-ray intensity incident on the scatterer.

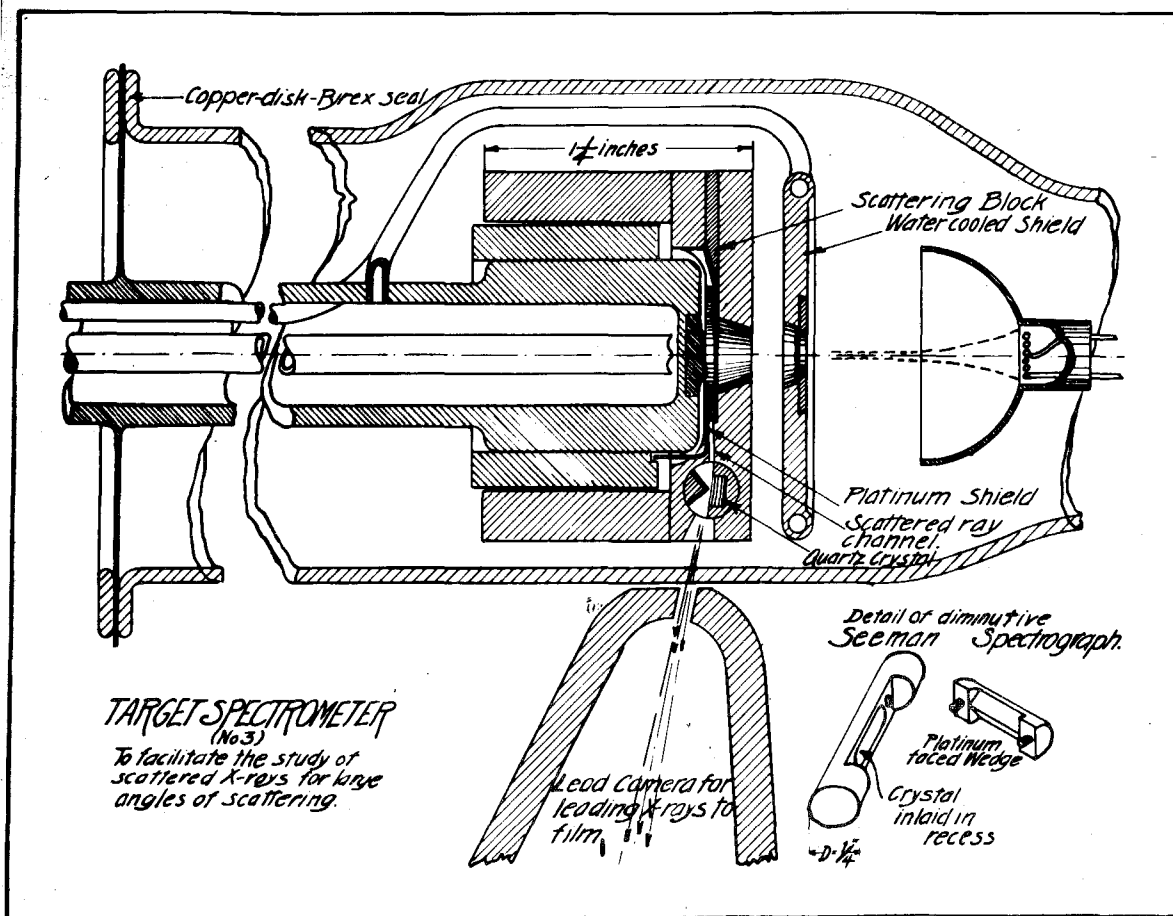


Fig. (2)

THE TARGET SPECTROMETER.

The "Target Spectrometer" shown in Fig. (2) was developed to meet the general requirements and difficulties of the problem just discussed. Four such spectrometers were built during a period of two years before a satisfactory design was obtained.

Some of the difficulties encountered were,

1. Maintaining the box containing the crystal and scatterer sufficiently cool not to damage either of these.
2. Developing an adequate seal and support for the heavy target structure.
3. Avoiding pitting of the molybdenum button with consequent cutting off of the radiation from the focal spot to the scatterer.
4. Avoiding evaporation of the molybdenum and its subsequent deposition on the scatterer.
5. Holding electrical conditions constant over long continuous exposures.
6. Insuring that the radiation studied came from the scatterer only.
7. Alignment of the camera.
8. Maintenance of high vacuum for long periods.
9. Avoiding shifting or vibration of the spectral image on the film during prolonged exposures.
10. Focusing the electron stream from the cathode on the opening of the target spectrometer box.

At the start great pains were taken to minimize the effects of electrons reflected from the focal spot of the target. It was feared that these would excite general radiation as they struck the scatterer and that this general radiation would completely

mask the effect sought. To avoid this the tube was originally designed with the target spectrometer box supported upon the target with several millimeters clearance by means of six insulating quartz studs. The box was then held at a potential intermediate between cathode and target of such a value that the short wave limit of the continuous spectrum due to the bombardment of the scatterer by reflected electrons fell outside the region to be studied. The intermediate potential was maintained through a third wire sealed in through the wall of the tube and connected at the proper point in a long high resistance shunted across the tube consisting of tap water running through a considerable length of glass tubing. These precautions were found upon trial to be entirely unnecessary and were abandoned in subsequent designs.

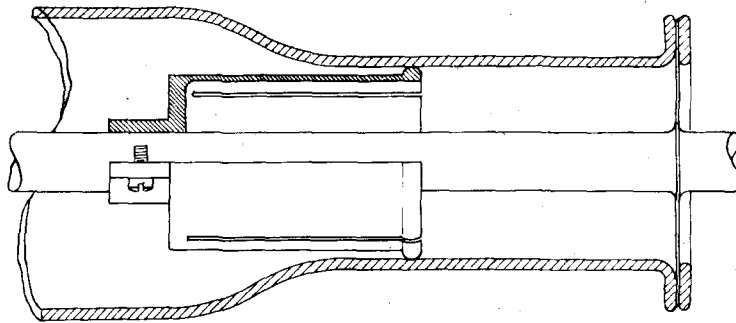
DETAILS OF TECHNIQUE.

The methods of overcoming the difficulties listed above will now be taken up in the order in which the difficulties were numbered.

1. Cooling. The tap water for cooling the tube was lead in through a length of 9 meters of $\frac{1}{4}$ inch glass tubing in the shape of a zigzag supported on a varnished redwood frame and the water discharged from the tube was led back to the grounded drain through a similar glass zigzag supported on the same frame. This arrangement permitted the water cooled anode of the tube to be raised to 30 K.V. above ground with only a small current leak back through the cooling water. The tube could thus be operated with ground potential half way between the potentials of anode and cathode.

It was found that even with the cathode beam well focused inside the hole provided for it in the target spectrometer box sufficient heat was developed by stray electrons impinging on the box to melt an aluminum scatterer and seriously damage the box. A shield shown in Fig. (2) was therefor provided and kept cool by means of auxiliary copper tubing brought in through a hole in the water cooled anode and soldered to the latter with silver solder. One end of this tubing opened directly into the hollow anode while the outlet end was lead outside the tube through the anode alongside the main anode intake tube. The cooling water thus had two parallel paths and to insure that flow was maintained in both simultaneously small glass Venturi tubes were employed in the two parallel water circuits just before these recombined to discharge through the long glass zigzag. Many exposures lasted more than a week running night and day. Any stoppage of the cooling water would result in destruction of the tube and to prevent this a protective device operated by the water pressure at the intake end of the glass zigzag was used. This consisted of a length of expansible copper "Sylphon" tubing arranged to hold open an electrical contact against the pressure of a spring when water pressure was admitted to the Sylphon. If the water was accidentally cut off the closing of the electrical contact threw a short circuit across a pair of electrical circuit breakers in the mains supplying current to the entire set. A breakage in the glass intake zigzag would have the same effect since the pressure in the sylphon could only be built up sufficiently by the hydrodynamic resistance in both intake and outlet zigzags.

2. The seal. The first models of the target spectrometer tube were made with soda glass walls. The seal in this case was made directly to the thin platinum cone silver soldered on the copper stem of the targets manufactured by the General Electric Co. In the course of modifying the original design tubes were blown in irregular assymetrical shapes. One of these for example had a large dome shaped protuberance containing a magnetic vane which could be rotated from the outside by a magnet and which transmitted an axial sliding motion to the target spectrometer box so that the angle of scattering could be varied at will. All the tubes had to be provided with a depression in the glass on the side where the spectrum issued from the tube and entered the camera. This depression permitted close approach of the small opening in the camera to the small opening in the spectrometer box inside the tube. Without such close approach general radiation would filter into the camera and fog the exposure. It was found very difficult to sucessfully blow, assemble and seal such complicated and irregular tubes when soda glass was used. Also the baking out temperatures during evacuation could not be raised to satisfactory values without danger of collapse with soda glass. For this reason the last two models were built of pyrex glass and a large disc of copper silver soldered to the stem of the target was used as the seal. It was necessary to make the silver soldered joint after the glass to copper joint as the silver melted at lower temperature than pyrex glass. To maintain the heavy target and spectrometer box accurately aligned in the tube so that the cathode rays would always enter the hole provided for them, a special steel cylindrical liner not shown in figure (2), was constructed in two

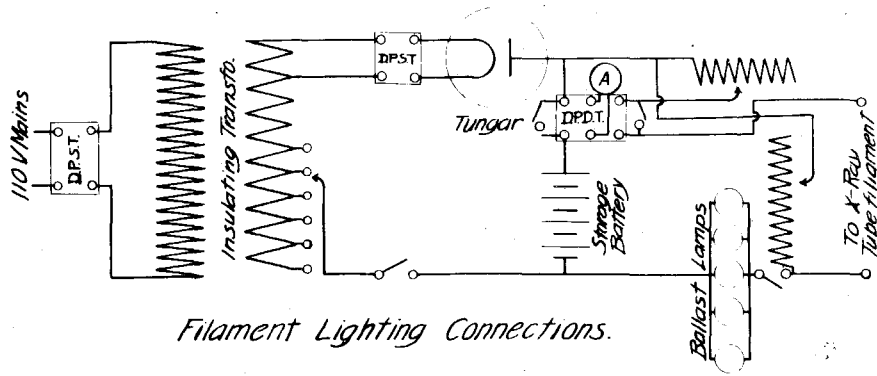


Half Section View of Liner.

Fig. (3)

halves to be fitted to the stem of the target at the proper stage in the assembly. A cross section of this liner is shown in Fig. (3). Slots cut in the cylindrical walls of this liner made it possible for the liner to be in elastic contact with the glass walls without danger of breaking them.

3. and 4. The pitting and evaporation of the target material were found to be very troublesome, Through a small hole in the scatterer described below the surface of the target could be examined without opening the tube by means of a short focus telescope. When serious pitting and sublimation on the scatterer had occurred this would be detected also with a fluoroscope by a considerable reduction in the intensity of X-rays filtering out through the scatterer. By experiment in this way it was found unsafe to run the tube with more than 10 m.a. at 50 K.V. As the efficiency of production of X-rays is proportional to the voltage the great advantage of high voltages is apparent when this limitation is placed on the power input. On the other hand exposures are at best so long and expensive (the continuous use of liquid air was required to maintain vacuum) that the tube had to run as near the safe limit as possible. Great difficulty was encountered maintaining the current constant at 10 m.a. for a week at a time without momentary increases which would instantly ruin the tube. The current through the tube depends very sensitively on the temperature of the cathode filament and hence on the current supplying that filament. Exposures were too long to permit the use of storage cells alone for this purpose and the filament was supplied with alternating current through an insulation transformer whose primary was connected to the supply mains.



Filament Lighting Connections.

Fig. (4)

Fluctuation in voltage of the supply mains of as much as 10% between night and day at the most diverse and unexpected times were encountered. These were quite sufficient to produce fluctuations of many milliamperes in the tube current and on several occasions several months work was ruined in a few seconds in this way. An induction voltage regulator was resorted to to maintain constant supply voltage at first but subsequently a better method was found.

5. Method of holding constant tube current. This consisted in supplying the filament of the tube with current from a battery of storage cells through a set of "ballast lamps". These ballast lamps through change in their resistance with temperature tend to maintain constant current. The battery of storage cells was maintained in a fully charged state at all times by current from an insulating transformer rectified by a tungar bulb. Resistances both in series and in parallel with the tube filament permitted adjustment of the tube current in spite of the constant current characteristic of the ballast lamps. Fig. (4) shows the connections diagrammatically. This scheme has proved most stable and satisfactory.

6. To insure that the spectrum incident on the film represents radiation coming only from the aluminum scatterer, four possible sources of trouble must be eliminated. First the crystal must be so oriented by turning the small cylindrical housing that the spectral region to be studied (about 100 X.U. on each side of $M\alpha$) comes exactly from the center of the scatterer. This was accomplished at the proper stage in the assembly of the tube while the target spectrometer was still accessible by temporarily removing the scatterer and covering the outside end of the scatterer

chamber with two tiny lead foil sheets so as to define a narrow slit exactly in line with the center of the scatterer. X-rays from another molybdenum tube were then caused to pass through this slit and fall on the Seeman Spectrograph on the opposite side of the target spectrometer box. The cylindrical crystal housing was then oriented by means of a long lever engaging in a small hole provided for this purpose until the line would be seen on a fluorescent screen placed in front of the target spectrometer. When the proper setting was obtained the cylindrical crystal housing was clamped in position with set screws and a photograph of the $\text{MoK}\alpha$ line as reflected from the crystal was taken as a check. The spectral band of continuous radiation defined by the width of the narrow slit between the two lead leaves across the scatterer opening could plainly be seen on these exposures and it was generally possible after a little practice to set the crystal so precisely that the $\text{MoK}\alpha$ line would fall quite accurately in the center of this region. The crystal used was a small piece of quartz the reflecting face of which was a very good natural surface and the other five faces were ground to fit the recess in the housing. The wedge was of copper faced with platinum and approached the face of the crystal having an opening of less than 0.1 mm. This combination gave extremely sharp lines. It was possible at a distance of 75 cm. to completely resolve the $\text{MoK}\alpha$ doublet whose separation is 4 x.u. .

Second, the direct radiations from the focal spot of the tube must be thoroughly screened from the crystal and from the opening of the camera. This was accomplished by means of the small piece of heavy sheet platinum bent into an L shape shown in Fig. (2). The inward lip of this platinum sheet was carefully placed so that no stray electrons from the cathode ray beam

could impinge upon it and excite primary X-rays which might pass into the spectrograph. This sheet formed one of the walls of a shallow channel of rectangular cross section $\frac{1}{16}$ " x $\frac{1}{4}$ " down which the scattered radiation from scatterer could pass to the spectrograph but whose alignment prevented the passage of any direct radiations. The other face of the platinum prevented any direct radiation from filtering through the copper housing into the camera. As a further precaution the face of the target was turned off in the lathe to a depth of about $\frac{1}{16}$ " except for a button of molybdenum at the center about $\frac{1}{4}$ " in diameter. This projecting button was then filed off at an angle of about fifteen degrees facing away from the spectrograph and camera and toward the scatterer. The focal spot was in the center of this beveled face and of somewhat smaller diameter. Third, since the entire interior of the target spectrometer box is bathed in primary X-radiation the interior surfaces of copper will scatter X-rays of the same order of intensity as the scatterer. By careful attention to the geometrical design of this box, however, the possibility of any such scattered radiation from the copper interior getting to the spectrograph was completely eliminated.

Fourth, the glass walls of the tube and the outer surfaces of the target spectrometer box were found to be faint sources of X-rays during the operation of the tube. This was doubtless the result of stray and reflected electrons. This effect was minimized on the side toward the camera by bringing the glass wall as close as possible to the copper target spectrometer box. The slit shaped opening in the camera through which the spectrum from the tube entered was made as small as possible, about $\frac{1}{16}$ " wide

by $\frac{1}{4}$ " long to minimize the amount of stray radiation which could enter the camera. To further reduce the intensity of this stray radiation entering through the small opening in the camera diaphragms were disposed inside the camera so as to cut off all radiation not propagated in the same direction as the spectrum itself. One of these diaphragms was removable and the opening in it was provided with a thin piece of black paper opaque to visible light but transparent to X-radiations. In this way the camera could be loaded with bare film without danger of fogging by visible light entering through the small opening provided for the X-ray spectrum. This precaution was taken to avoid the scattering during prolonged exposures of X-radiation by a black paper envelope in close proximity with the film which would be much more serious than scattering by the black paper diaphragm 70 cm. away. In the final improved design the camera was built 25 cm. longer than the distance from crystal to film required. This extra length was provided to reduce the scattering from the rear end of the camera back onto the film. Also the wooden back pressing against the film to hold it in place was abandoned and replaced by a pair of metal spring clips holding the film by two of its opposite edges. Thus there was nothing behind the film except the lead back of the camera 25 cm. distant. This lead back could not be omitted as the slight general X-radiation in the room was found sufficient to fog the film during long exposures. Indeed, the author discovered by accident in this way that the Kenetron rectifier tubes used with in connection with the set were faint sources of X-rays even when run with ample filament heating current so as to exceed by a liberal margin the emission of the X-ray tube. It was decided

that this was due to defective vacuum in the Kenetrons.

7. Alignment of the Camera. The above mentioned precautions for screening off stray radiation (small camera opening and restrictive diaphragms) introduced difficulties in aligning the external lead camera with the spectrum emerging from the X-ray tube. It was very disappointing to find after a 100 hour exposure that the alignment of the camera had been faulty. To avoid this the scatterer was made in two equal halves with a slight opening between. The plane of this opening produced was at right angles to the wedge and the crystal and cut the wedge at its midpoint. Visible light could be projected through this opening from the scatterer side of the tube. This light was reflected on the crystal under the wedge in the same direction as the X-rays. Looking from the near end of the camera with the diaphragm and black paper at the front end removed, this light could be seen as a bright point in the center of the small front opening in the camera when the correct alignment had been attained.

8. and 9. Maintenance of high vacuum in the X-ray tube by continuous operation of diffusion pumps was not feasible because of the vibration due to the boiling mercury. During the long exposures, vibrations or jars causing shifting of the spectrum relative to the film were greatly to be feared. Also it was found that a higher vacuum could be maintained by baking out the tube with a side tube full of coconut charcoal heated to 350° C, then sealing off the pumps and keeping the charcoal in liquid air than by continuous operation of the pumps. As either method would have required liquid air the charcoal tube was to be preferred.

The danger of vibration during exposures was greatest at the time

when the liquid air had to be replenished, about twice a day. It was found safer to cautiously remove the bottle from the charcoal tube than to try to fill it in place with a syphon.

10. In the earlier designs the cathode beam was so large that a good proportion of the tube current went to the spectrometer box instead of entering the hole and impinging on the target itself. This caused excessive heating of the edges of the hole and great loss of useful intensity. In the design with insulated spectrometer box this waste current could of course be measured and was found to be 25% of the total current. The useless radiation excited around the edges of the hole could be observed with a pinhole camera and fluoroscope. This difficulty was finally corrected by enlarging the hole and by the use of a special sharp focus cathode kindly presented the author by Dr. Coolidge. of the General Electric Co. In the later models the edges of the defining hole in the water cooled shield were protected with molybdenum. The problem of aligning the cathode so as to aim the beam exactly in the center of this hole was purely a question of glass blowing technique. The success obtained by Mr. Clancey in this direction is a tribute to his skill and judgement.

EXPOSURES.

In all about forty exposures were made with the target spectrometer tube varying in exposure time from ten to 100 hours. One two-hundred hour exposure was made. Two different scattering materials, Aluminum and Beryllium, were used. Very satisfactory photographs of the Compton shifted radiation could be obtained in twelve hours with Beryllium, but fifty to one-hundred hours was barely sufficient with Aluminum. Of all the exposures made only six were considered good enough for study. The longer exposures

were subject to accidental shut-down at unexpected times frequently in the night due to many causes such as temporary cut off of the water supply, shut down of the electrical power with opening of the breakers when the power came back, premature evaporation of the liquid air followed by gas-out from the charcoal and an arc over in the tube, accidental flash-over in the high tension parts of the equipment. Many of these interruptions did no damage to an exposure but merely amounted to so much "time out". In order to ascertain the exact duration of an exposure subject to interruption at unknown times, a special eight day exposure clock was built and mounted on the main switch board. Beside the hour and minute hands, this clock was provided with a day hand. An alternating current magnet in this clock held open a detent as long as power was on the switch board but any interruption in the operation of the set opening the breakers would cut off power from the magnet and allow the detent to stop the balance wheel of the clock. If power merely was cut off and turned on again without opening the breakers the clock would stop and then start itself by the action of the detent. The clock was set at zero when an exposure began and indicated not time of day but net time of exposure.

ANALYSIS OF FILMS.

The films were analysed with a microphotometer constructed at this Institute and employing a bismuth-tin alloy thermo-couple presented to the Institute through the kindness of its constructor, Dr. Pettit of the Mt. Wilson Observatory. The microphotometer was provided with two sets of slits before and behind the film to be

analysed. The second slit greatly increases the sharpness of definition. The light from the source, a 6 volt street lamp running on storage batteries for constancy was condensed on the first slit. The image of this illuminated slit in turn was focused with a microscope objective on the film to be analysed. This image again was focused by a second microscope objective on the second slit which was carefully set parallel to the first slit and exactly in the center of the illuminated image. The light from the second slit was finally condensed and minified down by a large aspherical lens to a spot sufficiently small to be entirely received on the 1mm. diameter disc of the thermocouple. The principal requirements of this optical system were a long, narrow, intensely and uniformly illuminated slit image on the film and all of the light from this image concentrated finally on the 1mm. diameter disc. of the thermocouple. The author succeeded in obtaining slit images on the film 8mm. long, fulfilling these requirements. The long slit image was necessary on account of the prominence of film grain. The spectral lines on films were about 25 mm. high. The accidental fluctuations in the microphotometer curves caused by the grain of the film tend to be averaged out with a sufficiently long slit image without any loss of definition in the spectral curve itself. In practice, the slit image 8 mm. high was made to explore the spectral distribution in a number of different regions of the 25 mm. height of the lines on the films so as to obtain a number of different curves from the same film. The accidental fluctuations on these films were then further reduced by taking the numerical average

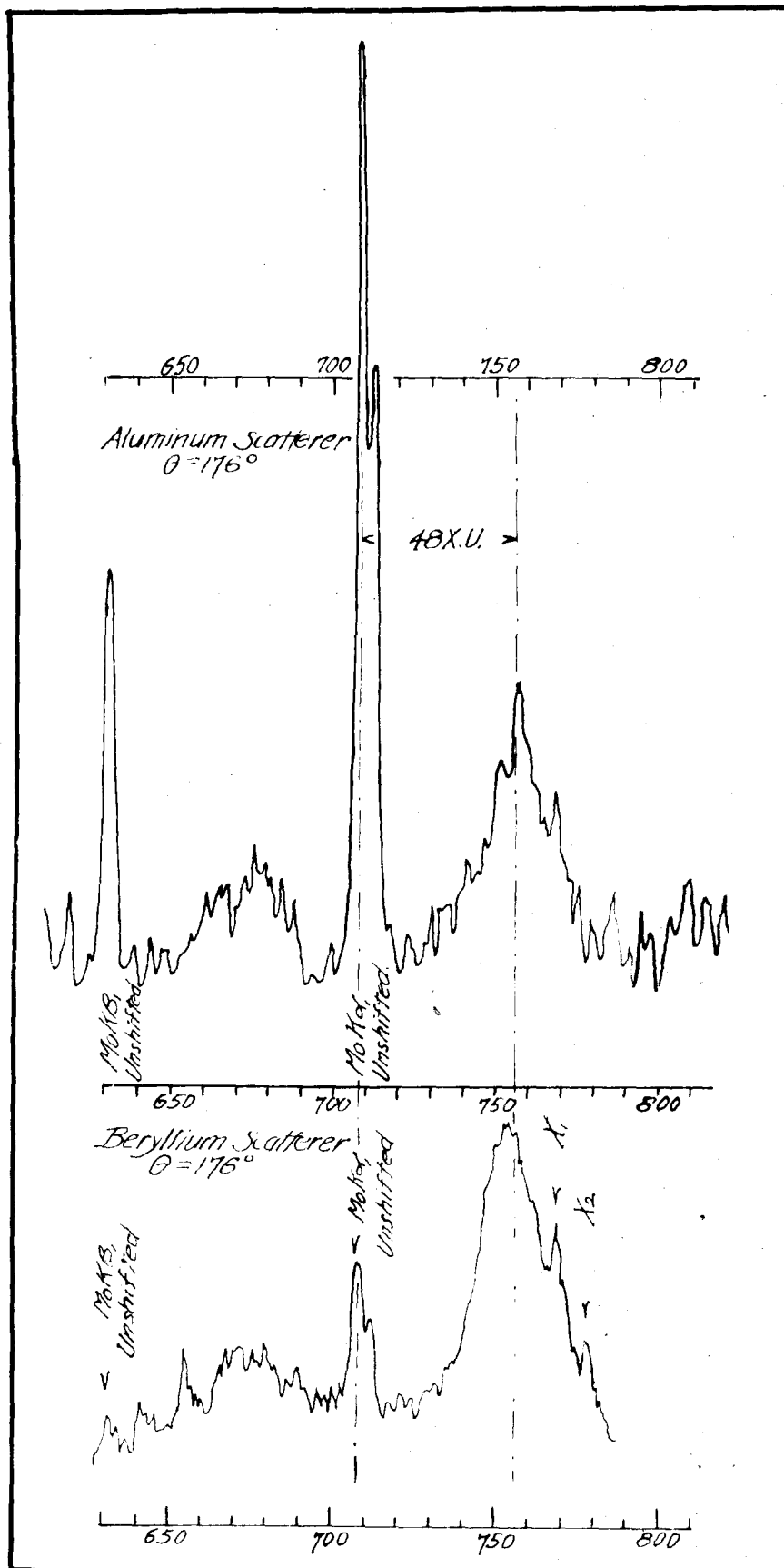


Fig. (5)

of the ordinates as read off the different curves. Ordinates were read at intervals of 1 mm. and in some cases every half mm. About 200 ordinates were generally read for each microphotometer curve. This was done by laying the plate on which the microphotometer curve appeared on a sheet of 1 mm. ruled cross section paper and estimating ordinate readings to 0.1 mm. The work was a little hard on the eyes but with a well arranged light and an ordinary reading glass it could be done quite rapidly.

The author wishes to express his deep appreciation of the valuable assistance given him in this part of the work with the microphotometer by Mr. Harry Kirkpatrick.

The spectral lines appear superposed on a rather heavy, smooth, continuous background. In the case of the curves from the aluminum scatterer, the background diminished rather rapidly in intensity toward longer wave lengths. To avoid the dissymmetry thus introduced in the line structure a smooth curve was drawn through the background with a spline and interpolated into the region of the Compton line. This curve was then subtracted from the observed line structure giving the curve shown in Fig. (5). This expedient was not necessary in the case of Beryllium as the background was sensibly uniform.

The Aluminum curve shown in Fig. (5) is the average of ten microphotometer curves taken on the best two films. The Beryllium curve is the average of these microphotometer curves taken on one film. In the case of Beryllium two other films were obtained, both being in general agreement with the one here shown. These two exposures were of longer duration than the one whose intensity curve is reproduced here. They were not used because they were

rather dense and some halation or mechanical shifting of the image, or both, was suspected. They showed both modified and unmodified line structure slightly broader than the one here reproduced in Fig. (5).

The relation between X-ray intensity and microphotometer deflection (ordinates of the curves) over the small range involved in the curves shown is closely linear. This was tested by means of calibration films on which appeared regions of blackening corresponding to equal steps of X-ray intensity taken from the spectral region near $\text{MoK}\alpha$. The equal steps were obtained by the use of an accurately cut exposure disc arranged to rotate rapidly on a motor shaft in front of the spectrum from a Seeman spectrograph so that in different regions of the film exposures of 0.1, 0.2, 0.3, etc. up to full exposure time were obtained.

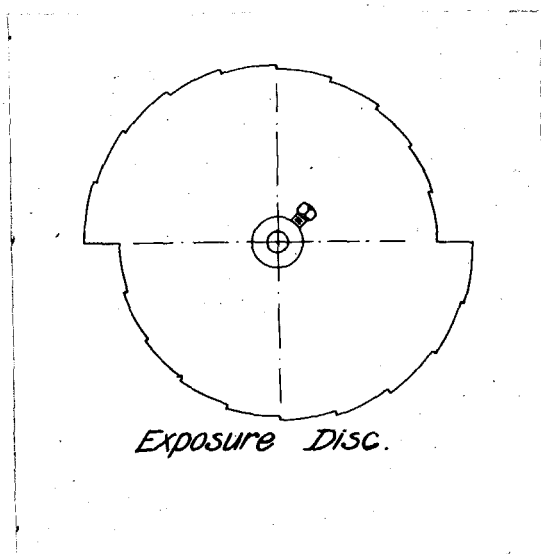


Fig. (6)

Fig. (6) shows the shape of this exposure disc. By trial exposures could be timed in such a way as to make the range of blackening on the calibration films ^{from} lightest to darkest overlap

the range of blackening of the Compton line films to be studied. staircase calibration curves were then run through the microphotometer from the calibration films immediately after running a curve on the Compton line without changing any of the constants or conditions on the microphotometer. It was found that over the same range of microphotometer deflections as that of the films of the experiment the scale was sensibly linear.

THE EXPERIMENTAL CURVES.

The author calls attention first to the breadth of the curves obtained for the spectral distribution of the Compton modified radiation as compared to the narrow unmodified $K\alpha_1$, and $K\alpha_2$ lines on the same curves. The scattering angle covered a range of inhomogeneity so near 180° that the broadening due to inhomogeneity of scattering angle is quite negligible. The first conclusion to be drawn is therefore that the process of scattering X-radiation by a solid scatterer (Aluminum and Beryllium) broadens the Compton line more than the unmodified line. A theory to explain this broadening effect is developed in the next section of this thesis.

The small peaks X_1 and X_2 in Fig. (5) are not yet definitely accounted for. They are perhaps fluorescence lines due to impurities in the Beryllium scattering block, possibly Strontium. If they correspond to Smeckal transitions such as those recently observed by Bergen Davis (Phys. Rev. p.331, Sept. 1928) one would be obliged to suppose energy level differences in Beryllium of much greater magnitude than we can yet explain. Moreover, the separation of X_1 and X_2 is about $8 \times U$. or about double the separation of the $K \alpha$ doublet of molybdenum. These lines appeared clearly in all the exposures made with the Beryllium

scatterer. The peaks in the Aluminum curve , although they resemble those of Beryllium, correspond to no very clearly defined lines on the film and it is safer to ascribe them to the accidents of film grain.

PART II.

THE RELATION BETWEEN COMPTON LINE STRUCTURE
AND ELECTRON VELOCITY DISTRIBUTION.

THE RELATION BETWEEN COMPTON LINE STRUCTURE AND ELECTRON
VELOCITY DISTRIBUTION.

The structure of the modified line is a key to the distribution of velocity of the electrons which scatter the modified radiation, the line being broadened by the random motion of these electrons in a way similar to that of the Doppler broadening of optical lines emitted by moving atoms. It is shown by means of certain approximative assumptions in an appendix to this paper that an ensemble of electrons all moving at one speed, v , in random directions will modify initially monochromatic radiation by scattering so as to give (as a first approximation) a spectral distribution consisting of a shifted rectangular band with a flat top and vertical discontinuous limits or edges,

see Fig. 7A.

The spectral width of the band is proportional to the speed v , of the electrons.

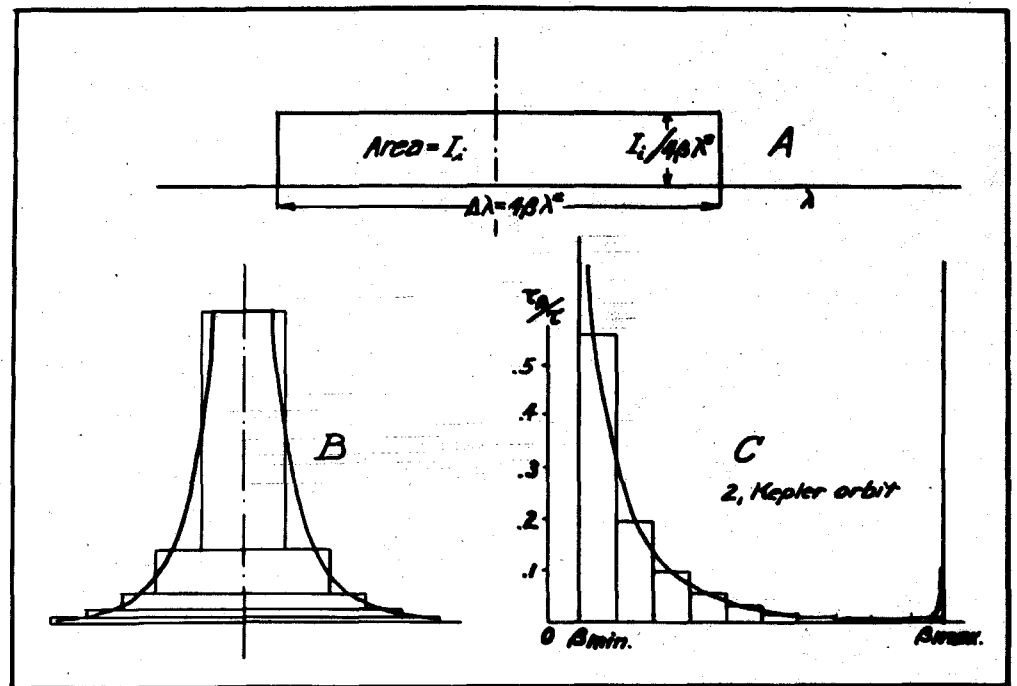


Fig. 7.

This band is nearly symmetrically distributed about the shifted position corresponding to free stationary electrons.

Throughout this paper the word "velocity" will be used to indicate a vector quantity, while the word "speed" will be used to indicate the absolute value of the velocity.

The approximation involves an error of the order of β^2 /unity (though β therefore need not be negligible compared to unity). In particular when the radiation is scattered at 180° or thereabouts, the width due to such an ensemble is shown

$$\Delta\lambda = 4\beta\lambda^*$$

where $\lambda^* = \lambda + \frac{h}{mc}$ and $\beta = \frac{v}{c}$, the speed of the electrons divided by the speed of light. (The theory presented here is completely non-committal as to the mechanism of this so called Doppler broadening and employs only the principles of conservation of energy and momentum. It is not therefore an attempt to explain the Compton effect on classical principles.) The area of the rectangular spectral band, Fig. 7 A, is proportional to the number of electrons in the ensemble and to the time during which they are exposed to the radiation if we assume that all electrons have the same a-priori probability of scattering (see footnote 12).

We shall therefore choose an area I_1 , corresponding to the area of the modified band produced by one ensemble of electrons, i having a standard population of say one electron per atom and corresponding to the total time of the exposure. The height of the corresponding rectangle is then given by $I_1/4\beta\lambda^*$. The choice of I_1 establishes the scale of ordinates (intensities) and is so chosen as to normalize the final total computed curve with respect to the area under the experimentally observed curve.

In order to compute the shifted distribution produced by all ensembles of electrons an assumption as to the relative a-priori probabilities of scattering by electrons in the different ensembles or classes must be made. We here assume these a-priori probabilities the same for all electrons.

With these considerations and assumptions we can compute a modified distribution for the scattered radiation from any atom model. For example, for a Bohr hydrogen-like model, having elliptical orbits, account can be taken of the variable velocity in the Kepler motion by a study of the proportionate times τ_p/τ spent by the electron in different speed ranges β to $\beta + d\beta$ between the maximum and minimum values β_{max}, β_{min} (perihelion and aphelion), where τ is the orbital period. The resulting distribution will be formed of infinitesimal elementary rectangles as shown in fig. 7B. The widths of rectangles are made proportional to the speeds, and their areas are given by $(\tau_p/\tau) I_\lambda$ so as to make the area of the total curved distribution equal to I_λ ,

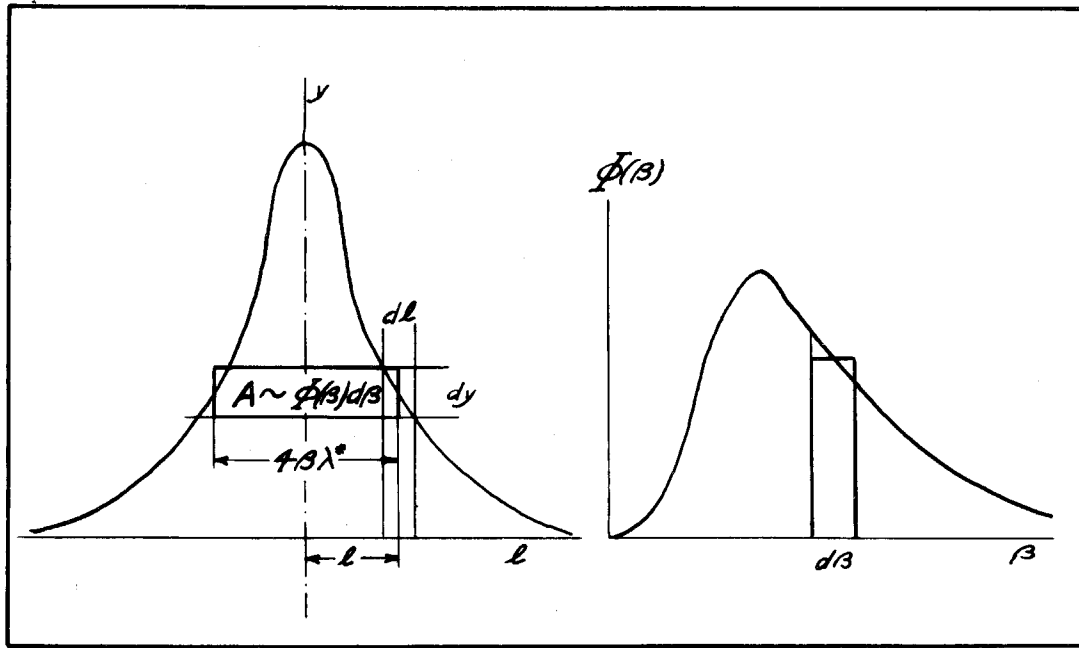
The height of each rectangle is given by $(\tau_p/\tau) I_\lambda / 4\beta\lambda^*$

5

5

This method of treatment is slightly different in form but identical in substance to the theory developed by G. E. M. Jauncey (Phys. Rev. 25, 314-322 (1925) 723-736 (1925)) for computing line structures due to electrons in Kepler orbits. It is developed in the form here given to permit of extension to wave-mechanical atom models. The author wishes explicitly to acknowledge his indebtedness to Dr. G. E. M. Jauncey.

The curve representing the shape or structure of the Compton modified line may then be obtained by assuming finite speed ranges and calculating finite rectangles to form a staircase distribution whose discontinuities are finally smoothed out by drawing a smooth curve as shown in Fig. 7B. Where practicable, however, it is better to obtain the



curve
by
the
following

Fig. 8

analytical method.

Referring to Fig. 8 a function $\Phi(\beta)$ is supposed given which expresses the probability of encountering an electron with speed between β and $\beta + d\beta$ as a function of β .

The electron ensemble having this speed β and randomly distributed velocity orientations contributes to the total line structure the elementary rectangle A whose area is proportional to $\Phi(\beta) d\beta$ and whose width is given as mentioned above by $4\beta\lambda^*$. The area of this rectangle is therefore

$$-2\ell dy = k \Phi(\beta) d\beta$$

where k is a constant determining the scale of y , and $\ell = \lambda' - \lambda - 2\eta_{mc}$ is the abscissa of the structure curve measured from its median point. $\ell = 2\beta\lambda^*$ and $\beta = \ell/2\lambda^*$ we can thus replace $d\beta$ by $d\ell/2\lambda^*$ and $\Phi(\beta)$ by $\Phi(\ell/2\lambda^*)$

The differential equation of the curve is given therefore by

$$-2\ell dy = k \Phi(\ell/2\lambda^*) d\ell/2\lambda^*$$

Dividing by -2ℓ and integrating this from $y=0, \ell=\infty$ to $y=y, \ell=\ell$ we obtain the equation of the line structure curve for continuous functions which vanish as $\ell \rightarrow \infty$

$$y = -k \int_{\ell=\infty}^{\ell=\ell} \Phi(\ell/2\lambda^*) d\ell/2\lambda^* \quad (2)$$

Formula (2) permits us either to start with an observed line structure and to deduce from this the electron velocity distribution function $\Phi(\beta)$ or to ^{start} with possible assumed velocity distributions $\Phi(\beta)$ and compute ideal line structures for comparison with the observed structure. The line structures so far determined are not sufficiently well defined to warrant the first mentioned procedure

but many interesting conclusions can be drawn by following the second.

GENERAL METHOD OF COMPUTING AND NORMALIZING LINE
STRUCTURE CURVES.

Each electron class (K, L, M, etc.) is assumed to contribute to the total line structure independently. Separate line structure curves are computed for each class of electrons. The ordinate scales are so chosen, as to make the area under each of these component curves proportional to the number of electrons responsible for that curve. These curves are then added to obtain the total line structure.

The primary radiation is not truly monochromatic but consists of a doublet ($K\alpha_1, K\alpha_2$). Mo $K\alpha_2$ is 4 X. U. longer in wave-length and half as intense as Mo $K\alpha_1$. In order to render the computed structure curves strictly comparable with the observed curves the following procedure was followed in all cases. The total structure curve was computed for a primary wave-length of 708 X. U. (Mo $K\alpha_1$) and the scale of ordinates was so chosen as to make the area under this curve equal to two thirds the area under the experimentally observed curve. This gives the contribution due to $K\alpha_1$. To this we add a precisely similar curve shifted however 4 X.U. in the direction of longer wave-lengths and having ordinates half as great as those of the first curve. This gives the contribution of $K\alpha_2$

The final curve has obviously an area just equal to the experimentally observed curve with which it is to be compared. By following this procedure no arbitrary assumptions need be introduced as to absolute intensities and the ordinate scale is uniquely determined.

The correction for the doublet character of the primary radiation above mentioned, introduces a plainly visible asymmetry in all of the computed curves.

ELECTRON VELOCITY DISTRIBUTIONS FOR WAVE MECHANICAL ATOM MODELS
AND DERIVATION OF THE CORRESPONDING LINE STRUCTURE CURVES

By means of the Dirac transformation theory it is possible to obtain the momentum distribution for a wave mechanical atom model given the space distribution (eigenfunction) for the same model. If p_1, p_2, p_3 , are the cartesian coordinates in the momentum space and x_1, x_2, x_3 , the cartesian coordinates in ordinary space then the probability of encountering a momentum (p_1, p_2, p_3) is given by the square of the absolute value of

$$\phi(p_1, p_2, p_3) = \iiint_{-\infty}^{+\infty} e^{-\frac{2\pi i}{h}(p_1 x_1 + p_2 x_2 + p_3 x_3)} \psi(x_1, x_2, x_3) dx_1 dx_2 dx_3 \quad (3)$$

The eigenfunctions used are those given by L. Pauling.⁶ An effective atomic number Z_i corrected for screening is computed for each class of electrons i and applied in the eigenfunction for that class. The author realizes that this is only a rough approximation which neglects mutual perturbations. An exact solution (if possible) would be very laborious and quite unwarranted for the purposes of this paper.

Equation (3) in polar coordinates becomes, if ψ is independent of θ' and ϕ' and depends on r alone

$$\phi(p) = \int_0^\infty \int_0^\pi \int_0^{2\pi} e^{-\frac{2\pi i}{h} p r \cos \theta'} \psi(r) r^2 \sin \theta' dr d\theta' d\phi' \quad (4)$$

⁶L. Pauling, Proc. Royal Soc. A114, 184 (1927).

$\phi(\rho)$ is generally a complex quantity. The square of its absolute value $|\phi(\rho)|^2$ gives the density in momentum or the probability of encountering an electron with momentum in the range between p_x, p_y, p_z and $p_x + dp_x, p_y + dp_y, p_z + dp_z$. The function $\Phi(\rho)$ which represents the probability of encountering an electron with momentum between $|\rho|$ and $|\rho| + d\rho$ is obtained by multiplying $|\phi(\rho)|^2$ by $4\pi\rho^2$

$$\Phi(\rho) = 4\pi\rho^2 |\phi(\rho)|^2$$

The resulting functions $\Phi(\rho)$ can be easily expressed as functions of β or ℓ by the relations

$$p = mv = m\beta c = mc\ell/2\lambda^*$$

The function $\Phi(\ell)$ thus determined is substituted in the formula (2) for the line structure curve. We tabulate below the electron class, the corresponding eigenfunction, and the resulting line structure curve function. Inessential multiplicative constants have been dropped since the line structure functions are to be subsequently normalized.

(K)	1, 0	$\psi_{1,0}(r) = e^{-\sigma_{1,0} r}$	$y_{1,0} = (1 + A_{1,0}^2 \ell^2)^{-3}$
(L)	2, 0	$\psi_{2,0}(r) = e^{-\sigma_{2,0} r} (-2 + 2\sigma_{2,0} r)$	$y_{2,0} = 2.5(1 + A_{2,0}^2 \ell^2)^{-3} - 7.5(1 + A_{2,0}^2 \ell^2)^{-4} + 6(1 + A_{2,0}^2 \ell^2)^{-5}$
(M)	3, 0	$\psi_{3,0}(r) = e^{-\sigma_{3,0} r} (6 - 12\sigma_{3,0} r + 4\sigma_{3,0}^2 r^2)$	$y_{3,0} = 4.701(1 + A_{3,0}^2 \ell^2)^{-3} - 37.612(1 + A_{3,0}^2 \ell^2)^{-4} + 110.328(1 + A_{3,0}^2 \ell^2)^{-5} - 133.731(1 + A_{3,0}^2 \ell^2)^{-6} + 57.313(1 + A_{3,0}^2 \ell^2)^{-7}$

$$\sigma_{n,\ell} = Z_{n,\ell} / na_0$$

$$\lambda^* = \lambda + h/mc = 732 \cdot 10^{-11} \text{ cm}$$

$$A_{n,\ell} = (2\pi a_0 n / Z_{n,\ell}) / (2\lambda^* h/mc)$$

$$a_0 = 5 \cdot 10^{-9} \text{ cm}, \quad h/mc = 24 \cdot 10^{-11} \text{ cm}$$

The effective atomic numbers applied to these functions are as follows: beryllium, $Z_{1,p} = 3.81$, $Z_{2,0} = 2$

LINE STRUCTURE CURVE DUE TO SOMMERFIELD CONDUCTION ELECTRONS.

By the application of the Fermi-Pauli statistics Sommerfeld has recently shown that the conduction electrons in metallic crystal lattices will have the following velocity distribution:

$$\Phi(v) = kv^2 \quad \text{when } |v| < V \quad (5)$$

$$\Phi(v) = 0 \quad \text{when } |v| > V \quad (6)$$

where V is given by

$$V = \frac{h}{m} \left(\frac{3n}{4\pi G} \right)^{\frac{1}{3}} \quad (7)$$

n being the number of metallic electrons per cc in the crystal lattice and $G=2$.

Expressing this in terms of l and substituting in the formula (2) for the line structure we obtain omitting a constant coefficient and using the indefinite integral

$$y = -\int l^2 \frac{dl}{l} + C \quad \text{for } |l| < 2\lambda^* \frac{V}{c} \quad (8)$$

since $y=0$ when $l = \pm 2\lambda^* \frac{V}{c}$

$$C = \frac{1}{2} (2\lambda^* \frac{V}{c})^2$$

or

$$y = \frac{1}{2} (2\lambda^* \frac{V}{c})^2 - \frac{1}{2} l^2 \quad \text{for } |l| < 2\lambda^* \frac{V}{c} \quad (9)$$

$$y = 0 \quad \text{for } |l| > 2\lambda^* \frac{V}{c} \quad (10)$$

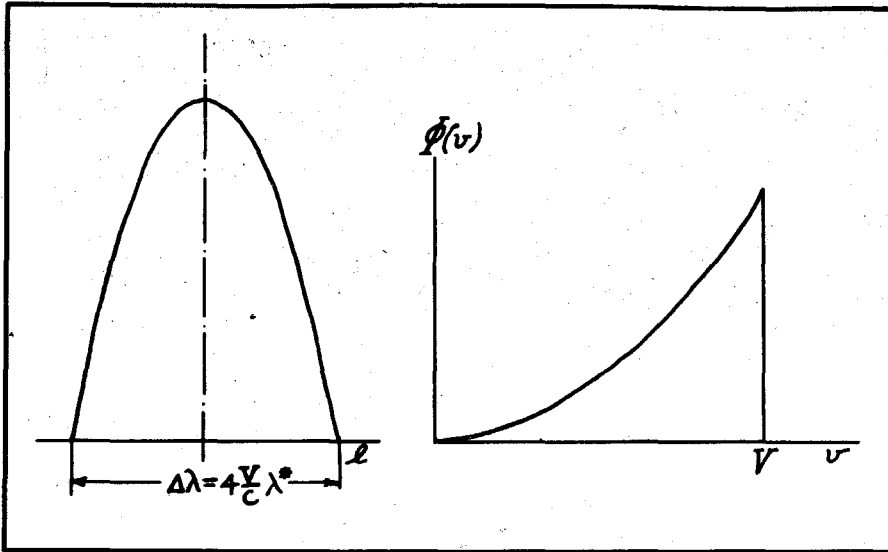


Fig. 9.

This is seen to be a line structure in the form of an inverted parabola of base width $4\lambda \frac{V}{c}$. Sommerfeld's electrons have much higher velocities than those required by classical statistics, and the result is a much broader

line structure. See Fig. 9.

LINE STRUCTURE CURVE DUE TO MAXWELL-BOLTZMANN DISTRIBUTION
OF CONDUCTION ELECTRON VELOCITIES.

This is obtained by the same method as the previous curves.

In this case

$$\Phi(v) = v^2 e^{-\frac{mv^2}{2kT}} = (cl/2\lambda^*)^2 e^{-\frac{m(cl/2\lambda^*)^2}{2kT}}$$

Substituting in the Eq. (2) and integrating

$$y = e^{-\frac{m(cl/2\lambda^*)^2 l^2}{2kT}} \quad (11)$$

This is a simple Gaussian error curve which for the temperature of the experiment has a width of only 0.4 X. U. at 1/e of maximum value.

LINE STRUCTURE CURVES FOR KEPLER ORBITAL VELOCITY DISTRIBUTIONS.

For the case of circular orbits since β is constant the distribution is evidently a simple rectangle as has been shown by G. E. M. Jauncey. Here $\Phi(v)$ degenerates into a simple vertical ordinate at the proper value of v .

For the case of elliptical orbits the function $\Phi(v)$ is of rather complicated form. For this reason the graphical method with finite speed intervals was resorted to. Fig. 7C shows a typical curve representing $\Phi(v)$ for a 2, orbit. The total speed range between maximum and minimum speed was divided into ten equal steps and the corresponding rectangles were plotted to obtain the component curves whose sum gave the structure curves shown in Fig. 10V. Attention is called to the general similarity existing between the structures due to wave mechanics and those due to the older Bohr-Sommerfeld Kepler orbits (see Fig. 10V and IIQ). The difference as would be expected is that the wave mechanics rounds off the sharp corners of the Kepler curves. The wave mechanics also permits some slight intensity at very large line breadths.⁷
This is doubtless the explanation for the existence of an unshifted line in cases where Jauncey's theory based on Kepler orbits called for no unshifted line.

⁷ The Bohr-Sommerfeld atom would also give a better fit if the azimuthal quantum number k were placed equal to $(l(l+1))^{1/2}$ however.

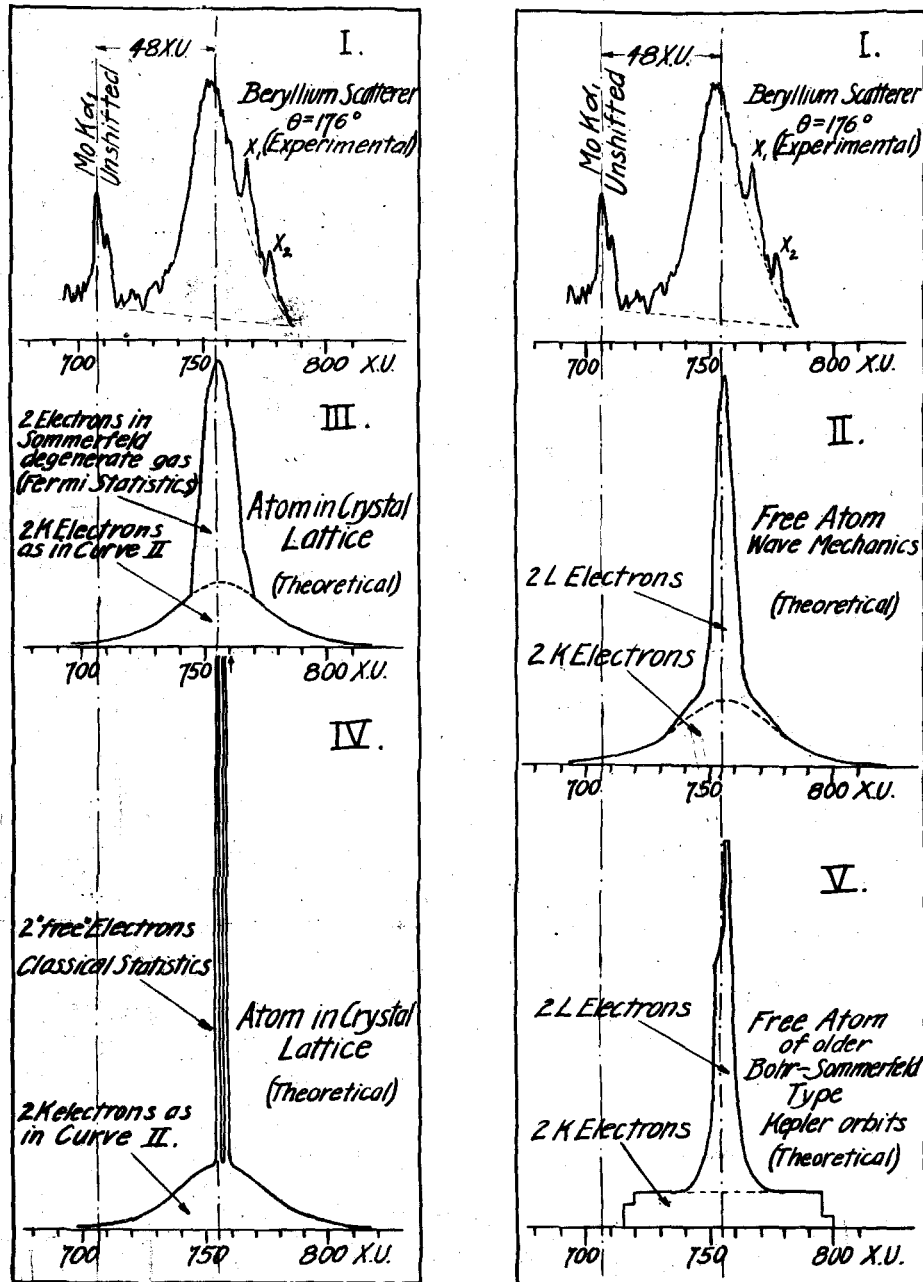


Fig.10.

CONCLUSIONS

It is evident from a comparison of the observed and computed line structures that the assumption of a class of electrons with velocities in agreement with the Maxwell-Boltzmann equipartition of thermal energy is untenable.

The two extremely tall and narrow peaks to, expected on this assumption are due to the $K\alpha_1$ and $K\alpha_2$ lines of the primary radiation and should be completely resolved as shown. We have in Curve (IV) Fig. 10, assumed the existence of two electrons per atom with such velocities. Even though this state were but one tenth or one twentieth as populous it would be easily detectable because of the narrowness of the curves called for by electrons with such slow velocities. Such narrow curves or peaks when normalized to give a total area equal to only a small fraction of the area under the observed curve would still have very appreciable ordinates.

The line structure to be expected from an atom with point electrons executing Kepler orbital motions with its resulting angularities and discontinuities is also seen to be discordant with the experimentally observed structure (compare Fig. 10V and I).

Of the two remaining, theoretical Curve III Fig. 10, corresponds to the assumption that the electron momentum is distributed as it would be in a free atom of beryllium and hence neglects the perturbing effect of the close proximity of the atoms in the crystal lattice. Curve II corresponds to the assumption that on account of the proximity of atoms two electrons per atom are not closely associated to any particular atom but constitute a degenerate electron gas while the remainder of the electrons are distributed in momentum as they would be in a free atom of beryllium neglecting the perturbing effect of neighboring atoms. This arbitrary division of electrons into two distinct classes is doubtless only a very rough approximation to the truth. It is highly probable that no sharp boundary divides the electron gas from the bound electrons there being an intermediate state in which electrons execute motions very different from those to be

expected in a single free unperturbed atom, but motions which nevertheless are to a large extent conditioned by the fields of one or more atoms. Such a class of electrons is neither completely free nor completely bound. It is difficult to take account of this intermediate class of electrons quantitatively⁸ but it is easy to see qualitatively the effect on the computed form of the line structure. Attention is called in Curve III Fig. 10, to the sharp breaks at the two points where the parabolic structure due to the electrons of the degenerate gas state meets the broad bell shaped structure due to the bound electrons. These breaks would certainly be absent if it were possible to take account of the continuous nature of the transition between the bound electrons and those in the degenerate gas state.

We now call attention to those parts of Curve II and III near the maximum. It is at once evident that Curve III is blunter and broader than Curve II and that in this respect Curve III is in better accord with the observed line structure. It is precisely in this portion of the curve that we should expect the degenerate gas approximation to give a good representation of the facts.

We may therefore conclude that the experimental curve supports the Sommerfeld theory of metallic electrons as a degenerate gas in just those regions for which this theory is designed to apply.

It is notable also that Curve III has a maximum ordinate slightly higher than that experimentally observed. Were Curve III to be corrected in order to take account of the continuous nature of the transition between the bound electrons and those in the degenerate gas state, it would be necessary to lower the maximum ordinate in order to maintain a constant area without changing the shape of the peak.

⁸ Bloch. Zeits. f. Physik, Jan. 1929.

This would doubtless improve the agreement of the observed and computed maximum ordinates.

To sum up our conclusions then we may say:

The Maxwell-Boltzmann statistics applied to conduction electrons give results discordant with the observed structure of the Compton line for scattering from beryllium.

The electron velocity distribution of the older Bohr-Sommerfeld atom model gives results discordant with the observed structure of the Compton line.

Velocity distributions based on the wave mechanics of a beryllium atom on the one hand and on the Sommerfeld theory of degenerate electron gas on the other give line structures in accord with the experimentally observed curves in the regions to which these theories are in each case designed to be applicable.

It is interesting to note that the conclusions drawn from this work constitute confirmatory evidence for the Sommerfeld theory of gas degeneration as applied to conduction electrons in a field of phenomena quite remote from that for which the theory was developed.

A simple computation shows that the recoil momentum taken by any electron in the case here discussed is sufficient to throw that electron completely out of the range of velocities forbidden by the presence of other electrons according to the Pauli "Verbot".

Work is now under way at this laboratory in an attempt to obtain experimental distribution curves with greater precision. A study of line structure scattered by nonconductors should prove interesting and is now being started. Work is being continued by the double crystal method of Bergen Davis and also by means of a multiple crystal spectrograph recently constructed here which permits the use of converging x-ray beams.

My sincere thanks are due to Professor W. V. Houston for his kindness in acquainting me with the results of the electron theory of metals in the Fermi statistics, and to Professor L. C. Pauling and Mr. Edwin McMillan for the help they have given me in the development and computation of the functions $\Phi(\beta)$ for wave mechanical atom models. I am much indebted to Professor Gregor Wentzel for his discussions and criticism in conversations in Paris and in subsequent letters. I am most grateful, also, to Professor R. A. Millikan for his faith and encouragement in this study which for a long time gave but meager promise of interesting results.

APPENDIX.

The explanation of Compton line breadth as a Doppler effect of the motion of bound and conduction electrons is an approximation. It has the advantage of offering a familiar pictorial explanation of the facts, but the disadvantage of limited applicability. To treat the problem rigorously one must set up a wave function for the crystal lattice and then compute the modified radiation by a method similar to that of G. Wentzel.⁹ This no one yet has succeeded in doing satisfactorily.

The present approximate theory is applicable to low electron velocities, long primary wave lengths and relatively free electrons or expressed precisely

$$v \ll c, \quad h/mc \ll \lambda, \quad E_B/E_R \ll 1 \quad (12)$$

E_B is the binding energy of the electron, E_R the energy received by the electron in the scattering process:

$$E_R = h\nu - h\nu' = hc(\lambda' - \lambda) / \lambda\lambda'$$

For any particular level the ratio E_B/E_R is evidently ^{a function} of λ the abscissa we have used in describing the line structure. It increases in the direction of shorter wave lengths but over the region $\lambda > 730 \times 10^{-10}$ does not exceed 0.2 for any level. For most levels it is very small indeed. The region $\lambda > 730 \times 10^{-10}$ includes all of the interesting portion of the modified line structure.

For any particular level the modified spectral distribution becomes discontinuous to the left of the point where the ratio $E_B/E_R = 1$. In this region the Smekal lines recently observed by Bergen Davis¹⁰ appear. The unshifted line may be considered as a special case of these. In the cases here discussed this region is too close to the unshifted line to be resolved.

The following assumptions which are all that are necessary for the derivations of formulas used in this paper seem justified for the region of approximation defined by the three inequalities (12).

(1). All electrons are assumed to have the same a-priori probability of scattering independent of their velocity or quantum state.

For the region defined above the classical scattering formula giving the total scattered intensity proportional to the total number of electrons for a wide variety of atoms is known to hold.¹¹

(2). Conservation of momentum and energy is assumed in the interaction of light quanta and electrons taking into account only the momentum and energy of the electron in the atom or in the crystal lattice just before scattering and similar quantities for the scattered quantum and the recoil electron. The modifying effect on the shifted radiation of any momentum or energy transferred or otherwise given to the rest of the atom in the scattering process is neglected.

9. G. Wentzel, Zeits. f. Physik 43, 2-8 (1927); 43, 779-787 (1927)

10. Bergen Davis, Phys. Rev. 32, 33 (1928).

11. Bergen Davis, Phys. Rev. 25, 737-739 (1925).

We first investigate the general case of an initially moving electron which scatters a quantum at an angle of scattering θ . Referring to Fig. 11, let ν_1 = initial frequency of quantum propagated in the direction of positive x-axis the interaction occurring at the origin. Let β_1, c be the speed of the electron before interaction a_1, b_1, c_1 , the direction cosines of its velocity and $a_1 = \cos \theta_1$, so that θ_1 is the angle between the electron's initial velocity and x-axis. Let the scattered quantum have a frequency ν_2 and a direction of propagation defined by the direction cosines p, q, r making angle ϕ with the initial velocity of the electron and an angle θ with OX. Then

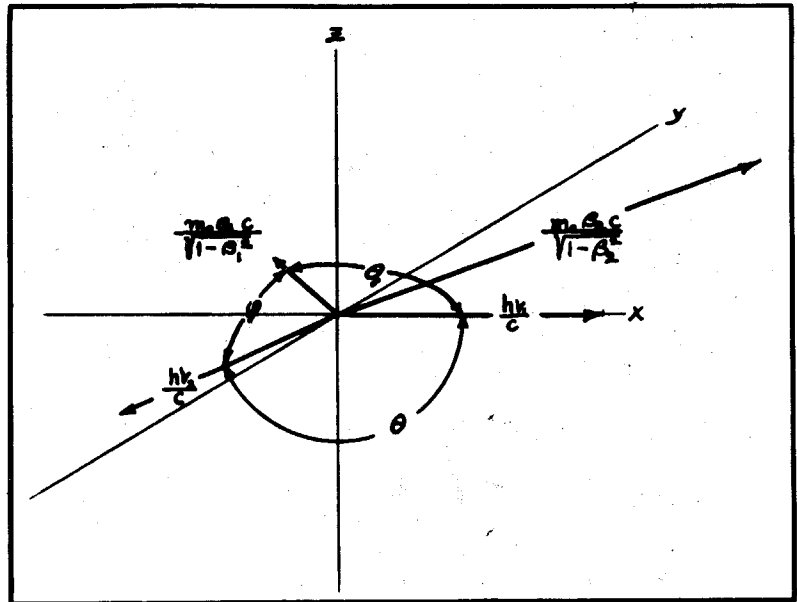


Fig. 11.

$$\cos \phi = (a_1 p + b_1 q + c_1 r)$$

$$p = \cos \theta$$

Let the recoil electron have a final speed $\beta_2 c$ in the direction defined by the cosines a_2, b_2, c_2 . (Cf., de Broglie "Ondes et Mouvements" Fascicule 1 pp. 94-95). Assumption (1) gives us the four equations.

$$\left. \begin{aligned} h\nu_1 + m_0 c^2 / (1 - \beta_1^2)^{1/2} &= h\nu_2 + m_0 c^2 / (1 - \beta_2^2)^{1/2} & (13) \\ h\nu_1 / c + [m_0 \beta_1 c / (1 - \beta_1^2)^{1/2}] a_1 &= (h\nu_2 / c) p + [m_0 \beta_2 c / (1 - \beta_2^2)^{1/2}] a_2 & (14) \\ [m_0 \beta_1 c / (1 - \beta_1^2)^{1/2}] a_2 &= (h\nu_2 / c) q + [m_0 \beta_2 c / (1 - \beta_2^2)^{1/2}] b_2 & (15) \\ [m_0 \beta_1 c / (1 - \beta_1^2)^{1/2}] a_3 &= (h\nu_2 / c) r + [m_0 \beta_2 c / (1 - \beta_2^2)^{1/2}] c_2 & (16) \end{aligned} \right\}$$

Eliminating a_2, b_2, c_2 and β_2 letting $\alpha = h\nu_1 / m_0 c^2$ we have

$$\nu_2 = \nu_1 \frac{1 - \beta_1 \cos \theta_1}{1 - \beta_1 \cos \phi + 2\alpha (1 - \beta_1^2)^{1/2} \sin^2 \frac{\theta}{2}} \quad (17)$$

Substituting $\nu = c/\lambda$ and neglecting β^2 in comparison to unity we have for the shift

(45)

$$\lambda_2 - \lambda_1 = \frac{\beta_1 (\cos \theta_1 - \cos \phi)}{1 - \beta_1 \cos \theta_1} \lambda_1 + \frac{2\alpha \lambda_1 \sin^2 \frac{\theta}{2}}{1 - \beta_1 \cos \theta_1} \quad (18)$$

in which the second term accounts for the simple "Compton Shift" and the first term represents the deviation from this shifted position caused by the electron's initial velocity. If now we substitute

$$l = \lambda_2 - \lambda_1 - 2\alpha \lambda_1 \sin^2 \frac{\theta}{2} \quad (19)$$

so that the new wave length coordinate l has for its origin the "center" of the shifted line (position for scattering by free stationary electrons) we obtain for the shift away from that new reference point

$$l = \frac{\beta_1 [\cos \theta_1 (\lambda_1 + 2\alpha \lambda_1 \sin^2 \frac{\theta}{2}) - \cos \phi \lambda_1]}{1 - \beta_1 \cos \theta_1}$$

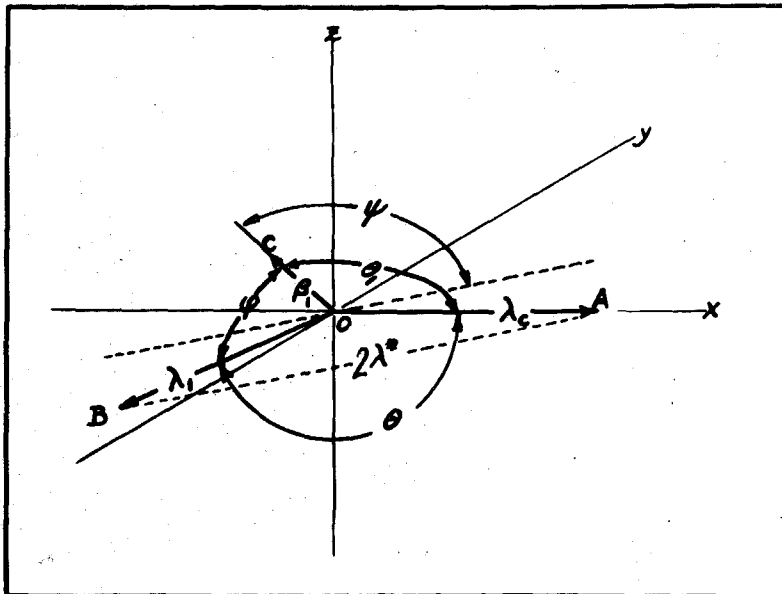
This can be considerably simplified by introducing a notation based on the special case of scattering by an initially stationary electron (Compton case).

Let the shifted wave-length for the Compton case be

$$\lambda_c = \lambda_1 + 2\alpha \lambda_1 \sin^2 \frac{\theta}{2}$$

then

$$l = \frac{\beta_1 \cos \theta_1 (\lambda_c - \beta_1 \cos \phi \lambda_1)}{1 - \beta_1 \cos \theta_1} \quad (20 a)$$



In Fig. (12) let OA be the direction of the incident quantum, OB the direction of the scattered quantum, OC the direction of the electron's initial velocity. We make the vector OA equal in length to λ_c and $|OB| = \lambda_1$. We define a new wave-length

$$2\lambda^* = (\lambda_c^2 + \lambda_1^2 - 2\lambda_c \lambda_1 \cos \theta)^{\frac{1}{2}}$$

represented in length by the vector AB.

Fig. 12.

We now note that the numerator in Eq.(20_a) can be represented in terms of the vectors of Fig.12, (designated by their termini) as the difference of two scalar products

$$C. A - C. B$$

or

$$C. (A - B).$$

Now the vector whose length is $2\lambda^*$ is precisely

$$(A - B).$$

Hence if ψ is the angle between OC and AB we have the identity

$$\beta_1 \cos \theta_1 \lambda_1 - \beta_1 \cos \phi \lambda_1 = 2 \beta_1 \cos \psi \lambda^*$$

so that we can write

$$l = \frac{2 \beta_1 \cos \psi}{1 - \beta_1 \cos \theta_1} \lambda^* \quad (20)$$

The direction AB is that of the vector difference between the momentum of the incident quantum and the momentum of the quantum scattered in the special Compton case of an initially stationary electron. It is evident that AB is the appropriate reference axis for the general case of an initially moving electron. The shift l is seen to be nearly proportional to the projection of the electron's initial velocity on this axis AB. It is important to note that this axis is fixed in space and that λ^* is a constant for any given angle of scattering θ and initial wave-length λ_1 .

In particular when the angle of scattering $\theta = 180^\circ$ or nearly so we have (the case of this experiment)

$$\cos \psi = \cos \theta_1 = -\cos \phi \quad (21)$$

$$l = \frac{2 \beta_1 \cos \theta_1}{1 - \beta_1 \cos \theta_1} \lambda^* \quad (21)$$

where $\lambda^* = (\lambda + h/mc)$

Holding β_1 , the initial speed of the electron constant and varying the directions of the electron's initial velocity defined by $\cos \theta_1$, it is evident from Eq.(21) that

$$-2 \beta_1 \lambda^* \leq l \leq 2 \beta_1 \lambda^* \quad \text{when } \beta_1 \ll 1 \quad (22)$$

or $-2 \beta_1 \lambda^* + 2 \beta_1^2 \lambda^* \leq l \leq 2 \beta_1 \lambda^* + 2 \beta_1^2 \lambda^*$ when β_1 is not small compared to 1 but $\beta_1^2 \ll 1$. l can therefore vary over the wave-length range given by:-

$$\Delta \lambda = 4 \beta_1 \lambda^* \quad (23)$$

for electrons of constant initial speed β_1 and varying directions θ_1

LINE STRUCTURE ELEMENT FOR AN ENSEMBLE OF ELECTRONS ALL
HAVING SPEED β AND RANDOM VELOCITY ORIENTATIONS.

An ensemble of electrons of the type mentioned is represented in velocity space by vectors radiating from the origin and having their termini distributed with uniform density over the surface of a sphere of radius β with the origin as center.

The probability of an encounter between a quantum and an electron such that the angle between the two trajectories is θ , (per unit small angular range $d\theta$) is

$$P_{\theta} = \frac{1}{2} \sin \theta, \quad (24)$$

The probability P_{ℓ} of a given shift, ℓ is obtained from equations (21), (24) and the derivative of (21) by eliminating θ , and $d\ell/d\theta$, as

$$P_{\ell} = (4\beta\lambda^*)^{-1} (1 + \ell/2\lambda^*)^{-2}$$

The error introduced by neglecting $\ell/2\lambda^*$ in comparison to unity is 3 per cent for $\ell = 25 \text{XU}$, $\lambda^* = 738 \text{XU}$, and much less for the more important parts of the line structure. Hence

$$P_{\ell} = 1/4\beta\lambda^*$$

and P_{ℓ} is thus seen to be independent of ℓ . Hence all shifts in the range permitted by inequalities (22) have the same probability, i.e. the distribution is rectangular.¹² (See Fig. 7A).

As indicated by inequalities (22) this rectangle is not quite symmetrically centered about the origin of wave-length abscissa ℓ for very large values of β but this slight correction has been neglected in the present paper.

12. This statement is strictly true if the ordinates of the distribution function or line structure curve are understood to represent the number of quanta. If the distribution curve represents the energy, however a slight correction for the variation in the energy per quantum over the breadth of the line is necessary. The computed curves of this paper represent the distribution of number of quanta as a function of wave-length and not the energy. The microphotometer curves on the other hand represent energy rather than number quanta. No correction was made for this, however, as the discrepancy thereby introduced is much smaller than the experimental uncertainties and in no way affects the conclusions.

SUMMARY.

An X-ray tube designed especially for the study of the Compton Effect at large angles of scattering has been developed. This tube contains both scattering substance and Seeman spectrograph in a small box inside the vacuum carried on the end of the anticathode. The spectral distribution of Mo K radiation scattered at very nearly 180° from metallic aluminum and beryllium scatterers has been studied with this tube and the following conclusion has been made :

The so-called Compton "shifted line" is a diffuse distribution with maximum intensity occurring at about the position required by the Compton formulae for shift after all experimental causes for such a breadth have been removed.

A theory for the diffuse character of this radiation has been developed based only on the assumptions of conservation of energy and momentum in elementary scattering processes which explains the observed breadth and structure in terms of the distribution of electron velocities in the metallic scatterer. An equation connecting electron velocity distribution and line structure has been derived making it possible to infer electron velocity distributions from observed line structures.

A comparison between theory and experiment leads to the conclusion that the conduction electrons in metals obey the Fermi statistics. The wave mechanical model for the bound electrons in the crystal lattice also appears more probable than the older type of Bohr-Sommerfeld atom with definite Kepler orbits.

REFERENCES.

- Bloch: Zeit. fur Physik, Jan. (1929).
- de Broglie: "Ondes et Movements", Fascicule 1 pp.94-95.
- Bergen Davis: Physical Review, pp.331, Sept. (1928)
- " " : Physical Review, v.32, pp.33 (1928).
- " " : " " , v.25, pp. 737-739 (1928).
- J.W. Dumond: Proc. Math. Acad., v.14, pp. 875-78, (1928).
- G.E.M. Jauncey: Physical Review, v.25, pp.315-322 (1925).
- " " , v.25, pp.723-736 (1925).
- G. Wentzel: Zeit. fur Physik, v.43, pp.1-8 (1927).
- " " " , v.43, pp. 779-787 (1927).